

Strain-induced crystal structure change in ultrathin films of $\text{Pr}_{0.7}\text{Sr}_{0.3}\text{MnO}_3$

Ian MacLaren^{a)} and Zhong Lin Wang^{b)}

Beijing Laboratory of Electron Microscopy, Chinese Academy of Sciences, P.O. Box 2724, Beijing 100080, People's Republic of China

H. S. Wang and Qi Li

Department of Physics, Pennsylvania State University, University Park, Pennsylvania 16802

(Received 22 October 2001; accepted for publication 27 December 2001)

Ultrathin films (<30 nm) of $\text{Pr}_{0.7}\text{Sr}_{0.3}\text{MnO}_3$ on LaAlO_3 have been studied using transmission electron microscopy (TEM). It was shown that the films are highly uniform and defect-free, and that they are coherently strained to the smaller lattice parameter of the substrate, resulting in a tetragonal expansion perpendicular to the film plane and a change of crystal structure from the ordered orthorhombic of bulk materials to a simple tetragonal perovskite. The variation of the tetragonality with distance from the interface was also determined from high-resolution TEM images. © 2002 American Institute of Physics. [DOI: 10.1063/1.1453482]

The discovery of large low-field magnetoresistance in ultrathin (<30 nm) $\text{Pr}_{1-x}\text{Sr}_x\text{MnO}_3$ (PSMO) films on LaAlO_3 substrates,^{1,2} as well as other interesting properties such as anisotropic magnetoresistance,^{3,4} strain-induced magnetic properties,⁵ and anomalous domain wall magnetoresistance,^{6,7} which are not reproduced in thicker films, has prompted interest into the possible mechanisms behind this change of properties in the very thinnest films.

Zandbergen *et al.*^{8,9} and Lebedev *et al.*¹⁰ have studied the structures of $\text{La}_{0.73}\text{Ca}_{0.27}\text{MnO}_3$ and $\text{La}_{0.9}\text{Sr}_{0.1}\text{MnO}_3$ films, respectively, deposited in both cases on the larger lattice parameter SrTiO_3 (STO) substrate, thus inducing a tensile strain in the plane of the thin films. For the very thinnest films ≤ 20 nm, which are coherently strained, both studies showed changes of the crystal structure from the normal bulk structure. In the case of $\text{La}_{0.73}\text{Ca}_{0.27}\text{MnO}_3$ on STO, the structure remained orthorhombic but with a loss of the octahedral tilting about the b axis that is normal for the bulk $Pnma$ structure. In the case of the $\text{La}_{0.9}\text{Sr}_{0.1}\text{MnO}_3$ on STO, the structure was altered from the bulk orthorhombic structure to a distorted rhombohedral or cubic structure, with a tetragonal distortion such that the unit cell is slightly flattened perpendicular to the film plane.

Lebedev *et al.*^{11,12} also studied the case of $\text{La}_{0.7}\text{Sr}_{0.3}\text{MnO}_3$ on LaAlO_3 , where the substrate has a smaller unit cell than the film and thus puts the film in compressive stress. In this case, ultrathin films also showed a change of crystal structure from the bulk orthorhombic to a structure that was either rhombohedral or cubic with a tetragonal elongation perpendicular to the film plane.

In this work, high-resolution transmission electron microscopy (HRTEM) imaging and selected area diffraction in the TEM is used to investigate the crystal structure and strain distribution in 30 nm thick films of $\text{Pr}_{0.67}\text{Sr}_{0.33}\text{MnO}_3$

(PSMO) grown on LaAlO_3 (LAO). These films are in compressive strain since the lattice parameter of PSMO is about 2% larger than that of LAO (the pseudocubic lattice parameters are 3.792 and 3.867 Å, respectively) and also show a tetragonal distortion and change of crystal structure as a result of the compressive strain.

Specimens of ultrathin (30 nm) $\text{Pr}_{0.67}\text{Sr}_{0.33}\text{MnO}_3$ films were produced by pulsed laser deposition on (001) LaAlO_3 as described previously.¹ Specimens for TEM observations were made by a standard cross-sectional preparation technique involving gluing two films face to face and then mechanically polishing and dimpling to a thickness less than 30 μm . This was followed by ion-beam thinning, taking care to ensure that the film was not preferentially thinned by the Ar ion beam. Transmission electron microscopy observations were made using a Philips CM200 FEG equipped with a Gatan imaging filter system, using diffraction contrast and high-resolution electron microscopy (HREM) imaging together with selected area diffraction (SAD).

Figure 1 shows a dark-field image of the film, showing fairly uniform bright contrast in the film, and weaker contrast in the substrate. This diffraction contrast imaging shows that the film was free of dislocations or other defects.

Figure 2 is a typical SAD pattern taken from both the film and the substrate, with the diffraction spots for the film arrowed. The spots are split in the direction perpendicular to the film plane with those for the film appearing inside those for the substrate, but there is no spot splitting in plane. Thus, the film is compressed in plane to fit to the smaller lattice

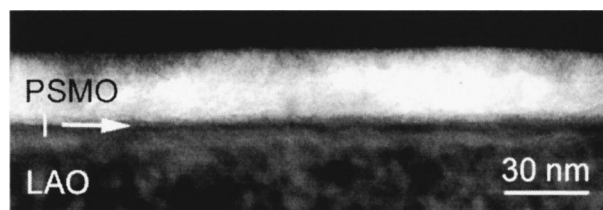


FIG. 1. Dark field TEM image of the PSMO thin film and LAO substrate, the interface is marked with an "I."

^{a)}Now at Max-Planck-Institut für Metallforschung, Seestr. 92, 70174 Stuttgart, Germany; electronic mail: ian.maclaren@physics.org

^{b)}Also at School of Materials Science and Engineering, Georgia Institute of Technology, Atlanta, GA 30332-0245.

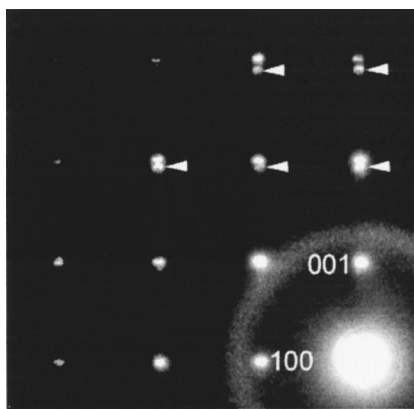


FIG. 2. SAD pattern of the PSMO thin film and LAO substrate with the spots for PSMO arrowed, 001 is perpendicular to the film plane and 100 lies in the film plane.

parameter LAO, and is tetragonally distorted out of the plane. The resulting c/a value has been calculated from four SAD patterns to be 1.034 ± 0.03 , which corresponds to a Poisson's ratio for the film of 0.36 ± 0.07 . These results are consistent with those of Wang *et al.*,¹³ where XRD was used to show that PSMO films on LAO were coherently strained and tetragonally distorted with a c/a of 1.042 giving a Poisson's ratio of 0.44. The slight discrepancy is perhaps understandable since in the preparation of a TEM cross-sectional sample, the thickness of the sample for TEM examination might change the interior strain slightly, possibly inducing a decrease in the constraint in the direction perpendicular to the sample plane, and there may therefore be some strain relaxation. On the other hand, the x-ray diffraction peaks, especially for in-plane directions, are broad for very thin films. This can also result in uncertainties in the determination of the lattice parameters.

Figure 3 shows a HREM image of a PSMO thin film and its interface to the LAO substrate (the film is somewhat thinner than 30 nm in this image as some of the surface was milled away in ion beam thinning). The interface is perfectly coherent and no misfit dislocations could be detected, in ac-

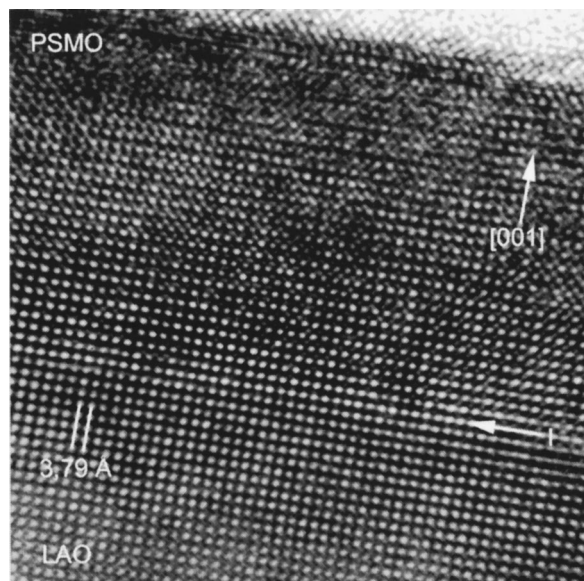


FIG. 3. HREM image of a PSMO thin film on LAO (defocus -88 nm), the interface is marked with an "I."

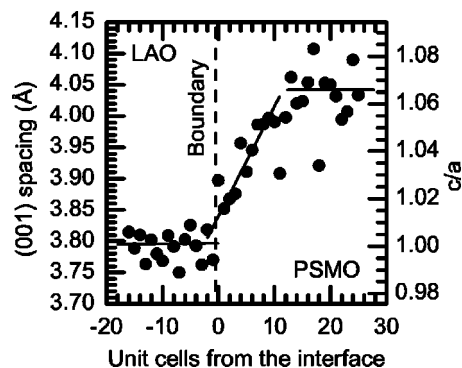


FIG. 4. Graph of the plane spacing and c/a ratio against the number of unit cells either side of the PSMO/LAO interface.

cordance with the SAD results. One surprising feature of this image, however, is that no evidence is found of the expected image contrast for the bulk orthorhombic unit cell of PSMO.¹⁴ Such a unit cell usually produces a period doubling in the images taken parallel to $[101]$ or $[10\bar{1}]$ such that 7.7 \AA (010) fringes are seen, or a rotation of the unit cell by 45° in images taken parallel to $[010]$ with 5.5 \AA spacing (100) and (001) fringes visible.^{15,16} Such fringes were never seen in any HREM images of this film and no superlattice spots for the orthorhombic phase could be found in SAD patterns or fast Fourier transforms (FFTs) of the areas in HREM images. Instead, all that can be seen corresponds to a simple perovskite unit cell. It would seem, therefore, that the influence of the high stress exerted by the film-substrate mismatch (about -2%) has promoted a tetragonal distortion and suppressed the cooperative tilting of the MnO_6 octahedra that leads to the formation of the normal bulk orthorhombic structure.

In order to determine the variation of tetragonal distortion with distance from the interface, a procedure was devised for processing this HREM image. The peaks in the HREM image were found using the NCEM peak analysis plug-in¹⁷ for the Gatan Digital Micrograph program. The peaks for each (001) plane were then fitted with a linear least-squares fit, and the distance between the midpoints of the fitted lines were taken as the average (001) plane spacings. The plane spacings could only be measured in this way for a limited distance from the interface, since too close to the film surface, random peaks due to amorphous material made accurate determination of the position of the (001) planes very unreliable. These plane spacings were then plotted against the number of unit cells from the interface in Fig. 4.

Although the results show significant scatter, some general trends can be discerned, as indicated by the thin lines on the graph. Immediately below the interface, the LAO substrate seems to be fairly undisturbed by the film and the (001) spacing remains close to its bulk value. In the first few layers of PSMO above the interface, the tetragonal distortion rises rapidly with distance from the interface. Above this, it appears to stabilize at a value between 1.06 and 1.07. It is unclear why the corresponding plane spacings ($>4 \text{ \AA}$) are rather higher than those reported by Wang *et al.*¹³ (3.93 \AA) or those determined by SAD above (3.92 \AA), although the fact that the other techniques give average values, whereas this shows that a variation with distance could provide a partial

explanation. It could also be that the (001) plane spacing is not so high for the whole 30 nm thickness of the film, since we have just measured the first 10 nm of the film.

Also, the precise reason why the tetragonality increases with distance from the interface for about 10 unit cells is unclear. Close to the interface, it *could* be that weaker near-neighbor interactions between the substrate and film may constrain the film somewhat in the *c* direction, but this effect becomes weaker as the distance from the interface increases. It may be noted that Lebedev *et al.*¹² have also noted a similar effect of increasing distortion with increasing distance from the interface by FFT processing of HREM images, although in this case it was in the substrate.

This change of structure in thin films from an orthorhombic structure having cooperative tilting of the MnO_6 octahedra to a simple tetragonal perovskite structure with all the octahedra aligned perpendicular to the interface would quite naturally have a huge influence on many relevant properties of these thin films. As one example, this would force all the magnetic Mn ions into the same alignment parallel to [001], which would probably have the effect of ensuring that the easy axis of magnetization lies in the out-of-plane orientation, as observed in previous work.⁵ It is, therefore, very important to take into account the possibility of stress-induced changes of crystal structure from the bulk crystal structure when seeking to understand the properties of ultrathin (<30 nm) films of manganite thin films.

The authors thank Professor K. H. Kuo for helpful discussions and support during the course of this work. The

work at the Beijing Laboratory of Electron Microscopy was performed with financial support from the National Natural Science Foundation of China (5982550), and at Pennsylvania State University was partially supported by NSF Grant Nos. DMR-9876266 and DMR-9972973.

- ¹H. S. Wang and Q. Li, Appl. Phys. Lett. **73**, 2360 (1998).
- ²H. S. Wang, E. Wertz, Y. F. Hu, and Q. Li, J. Appl. Phys. **87**, 6749 (2000).
- ³H. S. Wang, Q. Li, K. Liu, and C. L. Chien, Appl. Phys. Lett. **74**, 2212 (1999).
- ⁴Q. Li, H. S. Wang, Y. F. Hu, and E. Wertz, J. Appl. Phys. **87**, 5573 (2000).
- ⁵X. W. Wu, M. S. Rzchowski, H. S. Wang, and Q. Li, Phys. Rev. B **61**, 10259 (2000).
- ⁶Q. Li and H. S. Wang, J. Supercond. **14**, 231 (2001).
- ⁷Q. Li, Y. F. Hu, and H. S. Wang, J. Appl. Phys. **89**, 6952 (2001).
- ⁸H. W. Zandbergen, S. Freisem, T. Nojima, and J. Aarts, Phys. Rev. B **60**, 10259 (1999).
- ⁹H. W. Zandbergen, J. Jansen, S. Freisem, T. Nojima, and J. Aarts, Philos. Mag. A **80**, 337 (2000).
- ¹⁰O. I. Lebedev, G. Van Tendeloo, S. Amelinckx, F. Razavi, and H. U. Habermeier, Philos. Mag. A **81**, 797 (2001).
- ¹¹G. Van Tendeloo, O. I. Lebedev, and S. Amelinckx, J. Magn. Magn. Mater. **211**, 73 (2000).
- ¹²O. I. Lebedev, G. Van Tendeloo, S. Amelinckx, H. L. Ju, and K. M. Krishnan, Philos. Mag. A **80**, 673 (2000).
- ¹³H. S. Wang, E. Wertz, Y. F. Hu, Q. Li, and D. G. Schlom, J. Appl. Phys. **87**, 7409 (2000).
- ¹⁴K. Knížek, Z. Jiráček, E. Pollert, F. Zounová, and S. Vratislav, J. Solid State Chem. **100**, 292 (1992).
- ¹⁵O. I. Lebedev, G. Van Tendeloo, S. Amelinckx, B. Leibold, and H.-U. Habermeier, Phys. Rev. B **58**, 8065 (1998).
- ¹⁶C. J. Lu, Z. L. Wang, C. Kwon, and Q. X. Jia, J. Appl. Phys. **88**, 4032 (2000).
- ¹⁷R. Kilaas and S. Paciornik, part of the NCEM Image Processing Extension Package, available free from <http://ncem.lbl.gov/frames/software.htm>